Scientific Research Publishing

Open Journal of Polymer Chemistry, 2022, 12, 43-54
https://www.scirp.org/journal/ojpchem
ISSN Online: 2165-6711
ISSN Print: 2165-6681

Mechanisms of Cup-Shaped Vesicle Formation Using Amphiphilic Diblock Copolymer

Eri Yoshida

Department of Applied Chemistry and Life Science, Toyohashi University of Technology, Toyohashi, Japan
Email: yoshida.eri.gu@tut.jp

How to cite this paper: Yoshida, E. (2022) Mechanisms of Cup-Shaped Vesicle Formation Using Amphiphilic Diblock Copolymer. *Open Journal of Polymer Chemistry*, **12**, 43-54.
https://doi.org/10.4236/ojpchem.2022.122003

Received: March 11, 2022
Accepted: April 10, 2022
Published: April 13, 2022

Abstract

A cup shape is a dynamic morphology of cells and organelles. With the aim of elucidating the formation of the biotic cup-shaped morphology, this study investigated cup-shaped vesicles consisting of an amphiphilic diblock copolymer from the aspect of synthetic polymer chemistry. Cup-shaped vesicles were obtained by the polymerization-induced self-assembly of poly(methacrylic acid)-*block*-poly(*n*-butyl methacrylate-*random*-methacrylic acid), PMAA-*b*-P(BMA-*r*-MAA), in an aqueous methanol solution using the photo nitroxide-mediated controlled/living radical polymerization technique. Field emission scanning electron microscopic observations demonstrated that the cup-shaped vesicles were suddenly formed during the late stage of the polymerization due to the extension of the hydrophobic P(BMA-*r*-MAA) block chain. During the early stage, the polymerization produced spherical vesicles rather than a cup shape. As the hydrophobic block chain was extended by the polymerization progress, the spherical vesicles reduced the size and were accompanied by the generation of small particles that were attached to the vesicles. The vesicles continued to reduce the size due to further extension of the hydrophobic chain; however, they suddenly grew into cup-shaped vesicles. This growth was accounted for by a change in the critical packing shape of the copolymer due to the hydrophobic chain extension. These findings are helpful for a better understanding of the biotic cup-shaped vesicle formation.

Keywords

Cup-Shaped Vesicles, Polymerization-Induced Self-Assembly, Poly(methacrylic acid)-*block*-poly(*n*-butyl methacrylate-*random*-methacrylic acid), Critical Packing Shape

1. Introduction

Cup-shaped vesicles, often seen during cytosis, are a dynamic morphology of the

biomembrane. The vesicles play essential roles in material transport and energy metabolisms in the cytoplasm. Examples of cup-shaped vesicles include phagophores, which are formed during the early stage of autophagy to initiate the autophagous metabolism [1] [2] [3]. The phagophores take damaged organelles and harmful components into their cavity of the cup by extending their relative protein-poor membrane and form the closed phagosomes with a double membrane structure for catabolism and recycling of these useless organelles and components [4] [5]. Exosomes that are involved in exocytosis are also cup-shaped structures [6]. The exosomes transport materials, such as proteins, lipids, mRNA, and DNA, out of the cell for life activity maintenance and transmit information for cell-to-cell communication. These cup-shaped vesicles temporarily appear to play their roles, then disappear after finishing their tasks. However, the mechanisms of the cup-shaped vesicle generation have not been completely clarified, although the proteins and lipids participating in the cup-shaped vesicle formation have been discovered [3].

Synthetic cup-shaped vesicles have been prepared by the self-assembly of amphiphilic block copolymers, such as the poly(ethylene glycol)-*block*-polystyrene diblock copolymer [7] [8], poly[5-(*N*,*N*-diethylamino)isoprene] (PAI)-*block*-polystyrene-*block*-PAI triblock copolymer [9], and carbazole-supporting polystyrene (CzSt)-*block*-poly(ethylene glycol)-*block*-CzSt [10]. A random copolymer of the poly(methacrylic acid-*random*-styrene) [11] and a homopolymer of the carboxyl-terminated polyimide [12] also produced cup-shaped aggregates. Some of these vesicles serve in drug delivery as effective carriers that load drugs into the cavity of the cup [13]. The synthetic cup-shaped vesicles are also dynamic because they are the intermediates of their final structures, such as worm-like vesicles [14].

Micron-sized giant vesicles composed of amphiphilic poly(methacrylic acid)-*block*-poly(alkyl methacrylate)-*random*-methacrylic acid) produced unique artificial biomembrane models for cells and organelles based on many similarities to the biomembranes regarding their morphologies [15] [16], stimuli-responsiveness [17], and membrane permeability [18]. Examples of the models are the spherical vesicles with the erythrocyte-like morphology transformation [19], the perforated vesicles for the nuclear envelope [20], the villus-like structure [21], the anastomosed tubular networks following a fenestrated sheet for the endoplasmic reticulum and Golgi apparatus [22], the tubule extension from the vesicle surface for the neurons [23], and a polyelectrolyte that induces the budding separation for the membrane protein for endocytosis [24]. These models facilitated a better understanding of the biotic morphology formations. This study investigated the cup-shaped vesicle formation using amphiphilic poly(methacrylic acid)-*block*-poly(*n*-butyl methacrylate-*random*-methacrylic acid), PMAA-*b*-P(BMA-*r*-MAA), with the aim of elucidating the biotic cup-shaped vesicle formation from the aspect of synthetic polymer chemistry and molecular self-assembly. The PMAA-*b*-P(BMA-*r*-MAA) has been reported to produce flexible vesicles due to the butyl chain stretchiness [25]. This paper describes the formation and mechanism of

cup-shaped vesicles by the polymerization-induced self-assembly of this amphiphilic copolymer through the photo nitroxide-mediated controlled/ living radical polymerization (photo-NMP).

2. Experimental

2.1. Instrumentation

The photo-NMP was performed using an Ushio optical modulex BA-H502, an illuminator OPM2-502H with a high-illumination lens UI-OP2SL, and a 500W super high-pressure UV lamp USH-500SC2. ^{1}H NMR measurements were conducted using Jeol ECS400 and ECS500 FT NMR spectrometers. Gel permeation chromatography (GPC) was performed at 40˚C using a Tosoh GPC-8020 instrument equipped with a DP-8020 dual pump, a CO-8020 column oven, and a RI-8020 refractometer. Two gel columns of Tosoh TSK-GEL *α*-M were used with *N*,*N*-dimethylformamide (DMF) containing 30 mM LiBr and 60 mM H_3PO_4 as the eluent. Field emission scanning electron microscopy (FE-SEM) measurements were performed using a Hitachi SU8000 scanning electron microscope.

2.2. Materials

Methacrylic acid (MAA) was purified by distillation under reduced pressure. *n*-Butyl methacrylate (BMA) was passed through a column packed with activated alumina to remove an inhibitor and distilled over calcium hydride. BMA thus purified were degassed with Ar for 15 min with stirring just before use. 4-Methoxy-2,2,6,6-tetramethylpiperdine-1-oxyl (MTEMPO) was prepared as reported previously [26]. 2,2'-Azobis[2-(2-imidazolin-2-yl)propane] (V-61) and (4-*tert*-butylphenyl)diphenylsulfonium triflate (^{t}BuS) were purchased from Wako Pure Chemical Industries and Sigma-Aldrich, respectively and used as received. Methanol (MeOH) was refluxed over magnesium with iodine for several hours, and then distilled. Distilled water purchased from Wako Pure Chemical Industries was further purified by distillation. Extrapure Ar gas with over 99.999 vol% purity was purchased from Taiyo Nippon Sanso Corporation.

2.3. Preparation of PMAA End-Capped with MTEMPO

The PMAA end-capped with MTEMPO was prepared as reported previously [15] [27]; V-61 (22.8 mg, 0.0911 mmol), MTEMPO (18.0 mg, 0.0966 mmol), ^{t}BuS (24.0 mg, 0.0512 mmol), MAA (2.030 g, 23.6 mmol), and MeOH (4 mL) were placed in a 30-mL test tube joined to a high vacuum valve. The contents were degassed several times using a freeze-pump-thaw cycle and then charged with Ar. The polymerization was carried out at room temperature for 5.5 h with irradiation at 9.3 amperes with a 500W super high-pressure UV lamp using a reflective light from a mirror in order to avoid any thermal polymerization caused by the direct irradiation [28]. MeOH (11 mL) and distilled water (5 mL) degassed by bubbling Ar for 15 min were added to the product under a flow of Ar. After the product was completely dissolved in the aqueous MeOH solution, part

of the mixture (ca. 0.7 mL) was withdrawn to determine MAA conversion and the PMAA molecular weight. The conversion was calculated to be 76% by ^{1}H NMR. The solution withdrawn was poured into ether (50 mL) to precipitate the PMAA. The precipitate was collected by filtration and dried in vacuo for several hours to obtain the PMAA end-capped with MTEMPO (84.0 mg). The molecular weight (M_n) and molecular weight distribution (M_w/M_n) of the PMAA were M_n = 20,600 and M_w/M_n = 1.72, respectively, based on GPC calculation using PMAA standards. The degree of polymerization (DP) was 236 calculated using this molecular weight. The concentration of the PMAA in the resulting solution was 4.83×10^{-3} mol/L equal to the initial concentration of MTEMPO by a disregard for a slight contraction in volume due to the mixing of the methanol and water.

2.4. Photopolymerization-Induced Self-Assembly

The MTEMPO-capped PMAA solution containing unreacted MAA due to the 76% MAA conversion (4 mL containing 0.0193 mmol of the PMAA and 1.14 mmol of the unreacted MAA), BMA (563.2 mg, 3.96 mmol), and MAA (274.1 mg, 3.18 mmol) were placed in a 30-mL test tube joined to a high vacuum valve under a flow of Ar. The initial molar ratio of the monomers was MMA/MAA = 0.478/0.522. The contents were degassed several times using a freeze-pump-thaw cycle and finally charged with Ar. The polymerization was carried out at room temperature with a 600-rpm stirring speed by irradiation at 9.3 ampere using a reflective light. After the polymerization, part of the resulting dispersion solution (ca. 0.3 mL) was withdrawn to determine the monomer conversions. A mixed solvent (MeOH/H_2O = 3/1 *v*/*v*, 20 mL) was added to the dispersion solution to precipitate vesicles. The vesicles were cleaned with the mixed solvent by a repeated sedimentation-redispersion process. The resulting vesicles were stored in the presence of a small amount of the mixed solvent.

2.5. FE-SEM Observations

The vesicles were dried in air and subjected to the FE-SEM measurements at 1.0 kV without coating. Morphologies and size of vesicles were determined by the FE-SEM observations, while the size distribution was calculated as reported previously [29].

3. Results and Discussion

The polymerization-induced self-assembly of PMAA-*b*-P(BMA-*r*-MAA) was performed in an aqueous methanol solution (MeOH/water = 3/1 *v*/*v*) at room temperature through the photo-NMP of BMA and MAA using a PMAA end-capped with MTEMPO (**Figure 1**). The monomer conversions were estimated by ^{1}H NMR. The ^{1}H NMR spectrum of the copolymer is shown in **Figure 2**. The BMA conversion was estimated using the signal intensities for the ester methylene protons (COOC$\underline{H}_2$) of the monomer (**a**) and polymer (**b**), while the MAA

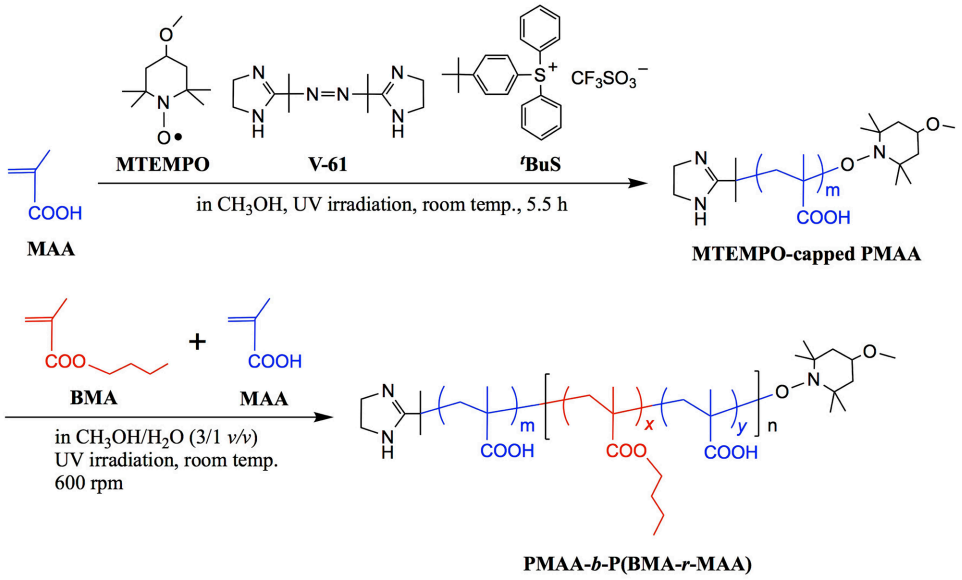

Figure 1. The photopolymerization-induced self-assembly of PMAA-*b*-P(BMA-*r*-MAA).

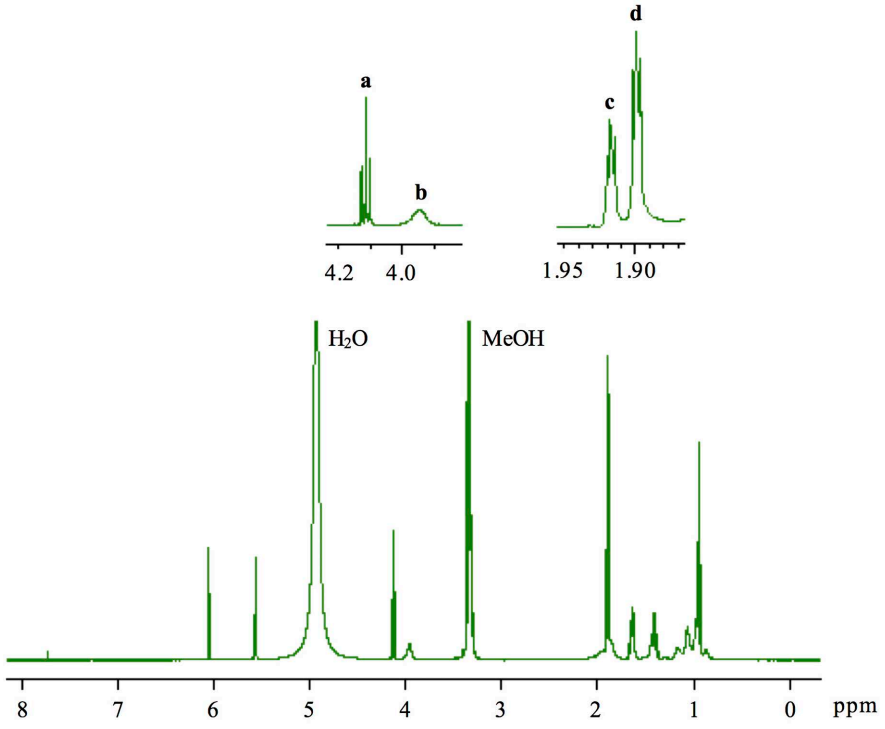

Figure 2. A ^{1}H NMR spectrum of the PMAA-*b*-P(BMA-*r*-MAA) and unreacted monomers. The polymerization: 5.5 h. Conversions: 55% for BMA and 28% for MAA. Solvent: $CD_3OD/CDCl_3$ = 3/1 *v*/*v*.

conversion was for the *α*-methyl protons (CH_2=C($C\underline{H}_3$)) of BMA (**c**) and MAA (**d**). **Figure 3** shows the time-conversion plots of the monomers and their first-order time-conversion plots coupled with the molar ratios of the monomer units during the polymerization. The first-order time-conversion plots showed a slightly negative deviation from a straight line for both monomers. The polymerization

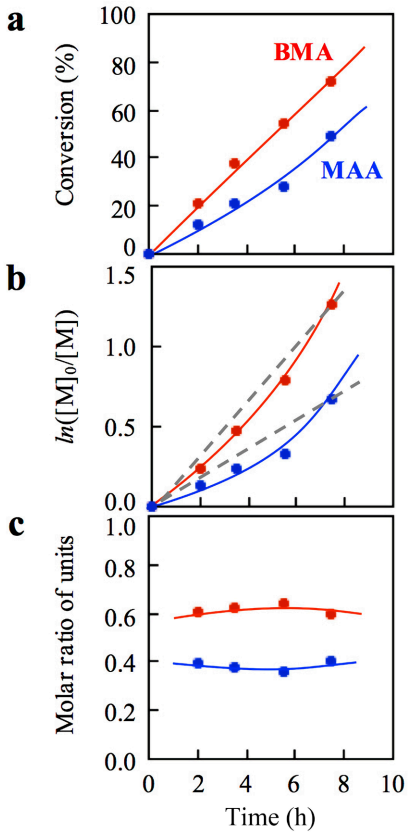

Figure 3. The variations in monomer conversions and molar ratios of the monomer units during the polymerization. (a) The time-conversion plots, (b) first-order time-conversion plots, and (c) molar ratios of the monomer units for the polymerization.

was accelerated during the late stage of the polymerization in the insoluble core phase formed by the self-assembling hydrophobic P(BMA-*r*-MAA) block chains. The polymerization produced a negligible change in the molar ratios of the monomer units for the random copolymer block throughout the polymerization. The molecular weight of the copolymer was determined by GPC based on PMAA standards. As shown in Figure 4, the GPC curve of the copolymer shifted to the higher molecular weight side with the reaction time. The molecular weight of the copolymer and DP of the P(BMA-*r*-MAA) block chain linearly increased with the BMA conversion, although the molecular weight distribution showed a slight increase with the conversion (Figure 5). The linear increases in the molecular weight and DP with the monomer conversion verified the living nature of the polymerization.

FE-SEM observations clarified the mechanism of the cup-shaped vesicle formation by the polymerization progress. Figure 6 shows the FE-SEM images of the vesicles for each BMA conversion. The vesicles were spherical rather than cup shaped during the early stage of the polymerization. The size of the vesicles decreased by the P(BMA-*r*-MAA) block chain extension (Figure 7). Some vesicles were joined to each other directly or via small particles, suggesting that they are structurally unstable. By further extending the hydrophobic chain, the

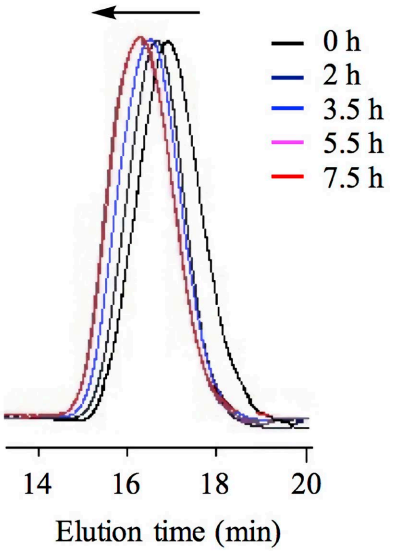

Figure 4. The GPC profiles of the copolymer for each reaction time.

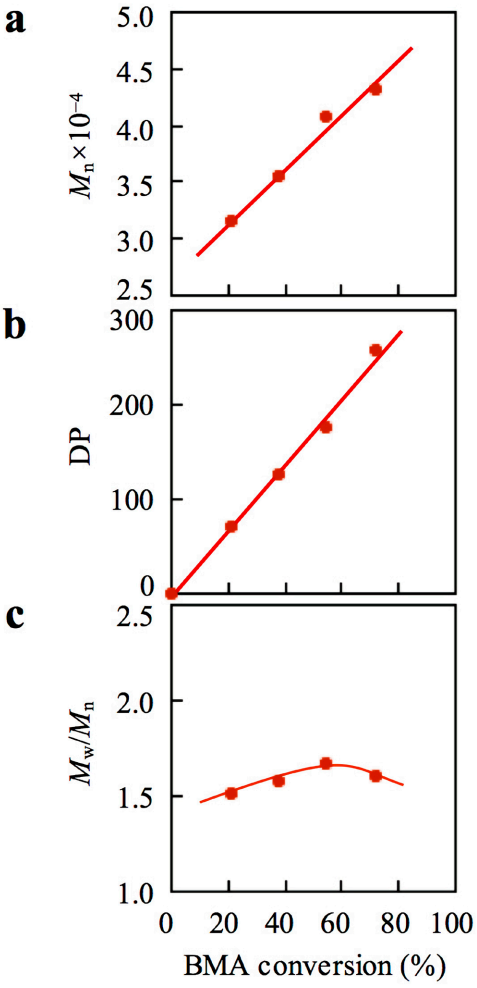

Figure 5. The living nature of the polymerization. The plots of (a) the molecular weight of the copolymer, (b) DP of the P(BMA-*r*-MAA) block chain, and (c) molecular weight distribution of the copolymer versus the BMA conversion.

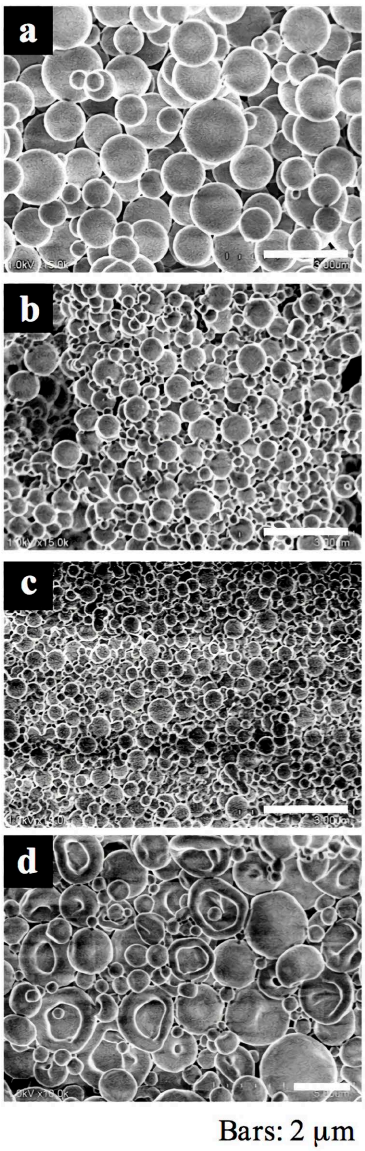

Figure 6. FE-SEM images of the vesicles for each BMA conbersion. The BMA conversion: (a) 21% (2 h), $PMAA_{236}$-*b*-$P(BMA_{0.609}$-*r*-$MAA_{0.391})_{72}$, (b) 38%, (3.5 h), $PMAA_{236}$-*b*-$P(BMA_{0.620}$-*r*-$MAA_{0.380})_{126}$, (c) 55% (5.5 h), $PMAA_{236}$-*b*-$P(BMA_{0.639}$-*r*-$MAA_{0.361})_{176}$, and (d) 72% (7.5 h), $PMAA_{236}$-*b*-$P(BMA_{0.593}$-*r*-$MAA_{0.407})_{257}$.

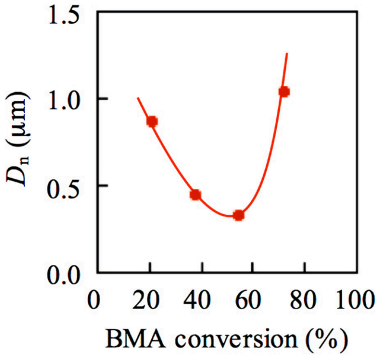

Figure 7. Plots of the vesicle size versus the BMA conversion.

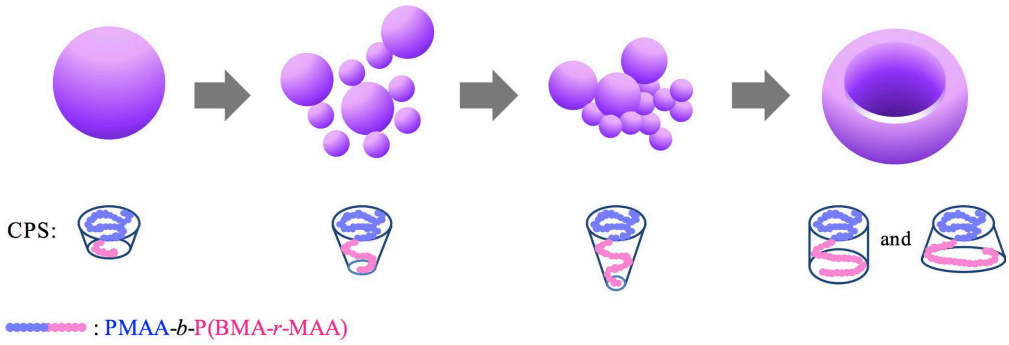

Figure 8. A schematic image of the growth into the cup-shaped vesicles and the critical packing shapes (CPS) of the copolymer.

vesicles were further connected to and fused with each other and accompanied by a continued decrease in size. These joined vesicles and particles suddenly grew into cup-shaped vesicles during the late stage of the polymerization. The size decrease and growth into cup-shaped vesicles can be accounted for by a change in the critical packing shape of the copolymer. A truncated cone-like shape during the early stage was changed into a cone-like shape by the hydrophobic block chain extension. A further extension of the hydrophobic chain increased the number of cylindrical shapes and inverted cone-like shapes, resulting in expansion of the surface area of the vesicles (**Figure 8**). It has been proposed for the phagophore formation that the phosphatidylethanolamine-containing proteins and phosphatidylinositol 3 phosphate-binding proteins alter the lipid composition of the source-derived bilayer to form phagophores [3]. These lipids of phosphatidylethanolamine and phosphatidylinositol 3 phosphate have inverted cone-like and cylindrical critical packing shapes, which extend the surface area and produce curvature of the bilayer membrane [30]. The sources of the bilayer are considered to be the endoplasmic reticulum and the outer leaflet of mitochondria rich in these lipids [31] [32]. The findings in this study indicate that the phagophore formation is caused by introducing these lipids into the source-derived lipid bilayer to produce the membrane curvature and extension.

4. Conclusion

Cup-shaped vesicles consisting of PMAA-*b*-P(BMA-*r*-MAA) were obtained by the polymerization-induced self-assembly. The polymerization was accelerated in the hydrophobic cores of the vesicles during the late stage; however, it had a living nature based on a linear increase in the molecular weight of the copolymer with the monomer conversion. The cup-shaped vesicles were formed during the late stage of the polymerization. The polymerization provided spherical vesicles rather than cup-shaped vesicles during the early stage. The spherical vesicles decreased the size by the hydrophobic block chain extension and were accompanied by the generation of small particles that joined the vesicles. By further extension of the hydrophobic block chain, the vesicles suddenly grew into cup-shaped vesicles during the late stage due to a change in the critical packing shape of the

copolymer. These findings in this study facilitated a better understanding of the phagophore formation. Fabrication of the dynamic morphologies similar to those of organelles using synthetic polymers is helpful in elucidating and better understanding the formation mechanisms of the biotic morphologies.

Acknowledgements

This work was supported by the JSPS Grant-in-Aid for Scientific Research (Grant Number 18K04863).

Conflicts of Interest

The author has no conflicts of interest in this study.

References

[1] Mizushima, N. (2007) Autophagy: Process and Function. *Genes & Development*, **21**, 2861-2873. https://doi.org/10.1101/gad.1599207

[2] Levine, B. and Kroemer, G. (2008) Autophagy in the Pathogenesis of Disease. *Cell*, **132**, 27-42. https://doi.org/10.1016/j.cell.2007.12.018

[3] Tooze, S.A. and Yoshimori, T. (2010) The Origin of the Autophagosomal Membrane. *Nature Cell Biology*, **12**, 831-835. https://doi.org/10.1038/ncb0910-831

[4] Fengsrud, M., Erichsen, E.S., Berg, T.O., Raiborg, C. and Seglen, P.O. (2000) Ultrastructural Characterization of the Delimiting Membranes of Isolated Autophagosomes and Amphisomes by Freeze-Fracture Electron Microscopy. *European Journal of Cell Biology*, **79**, 871-882. https://doi.org/10.1078/0171-9335-00125

[5] Lamb, C.A., Yoshimori, T. and Tooze, S.A. (2013) The Autophagosome: Origins Unknown, Biogenesis Complex. *Nature Reviews Molecular Cell Biology*, **14**, 759-774. https://doi.org/10.1038/nrm3696

[6] Rahmati, S., Shojaei, F., Shojaeian, A., Rezakhani, L. and Dehkordi, M.B. (2020) An Overview of Current Knowledge in Biological Functions and Potential Theragnostic Applications of Exosomes. *Chemistry and Physics of Lipids*, **226**, Article ID: 104836. https://doi.org/10.1016/j.chemphyslip.2019.104836

[7] Meeuwissen, S.A., Kim, K.T., Chen, Y., Pochan, D.J. and van Hest, J.C.M. (2011) Controlled Shape Transformation of Polymersome Stomatocytes. *Angewandte Chemie*, **123**, 7208-7211. https://doi.org/10.1002/ange.201102167

[8] Men, Y., Li, W., Janssen, G., Rikken, R.S.M. and Wilson, D.A. (2018) Stomatocyte in Stomatocyte: A New Shape of Polymersome Induced via Chemical-Addition Methodology. *Nano Letters*, **18**, 2081-2085. https://doi.org/10.1021/acs.nanolett.8b00187

[9] Riegel, I.C., Eisenberg, A., Petzhold, C.L. and Samios, D. (2002) Novel Bowl-Shaped Morphology of Crew-Cut Aggregates from Amphiphilic Block Copolymers of Styrene and 5-(*N*,*N*-Diethylamino)isoprene. *Langmuir*, **18**, 3358-3363. https://doi.org/10.1021/la015592t

[10] Li, G., Du, F., Wang, H. and Bai, R. (2014) Synthesis and Self-Assembly of Carbazole-Based Amphiphilic Triblock Copolymers with Aggregation-Induced Emission Enhancement. *Reactive & Functional Polymers*, **75**, 75-80. https://doi.org/10.1016/j.reactfunctpolym.2013.12.007

[11] Liu, X., Kim, J.-S., Wu, J. and Eisenberg, A. (2005) Bowl-Shaped Aggregates from the Self-Assembly of an Amphiphilic Random Copolymer of Poly(styrene-*co*-methacrylic acid). *Macromolecules*, **38**, 6749-6751. https://doi.org/10.1021/ma050665r

[12] Wang, J., Kuang, M., Duan, H., Chen, D. and Jiang, M. (2004) pH-Dependent Multiple Morphologies of Novel Aggregates of Carboxyl-Terminated Polymide in Water. *The European Physical Journal E*, **15**, 211-215. https://doi.org/10.1140/epje/i2004-10049-5

[13] van Rhee, P.G., Rikken, R.S.M., Abdelmohsen, L.K.E.A., Maan, J.C., Nolte, R.J.M., van Hest, J.C.M., Christianen, P.C.M. and Wilson D.A. (2014) Polymersome Magneto-Valves for Reversible Capture and Release of Nanoparticles. *Nature Communications*, **5**, Article No. 5010. https://doi.org/10.1038/ncomms6010

[14] Yoshida, E. (2016) Worm-Like Vesicle Formation by Photo-Controlled/Living Radical Polymerization-Induced Self-Assembly of Amphiphilic Poly(methacrylic acid)-*block*-poly(methyl methacrylate-*random*-methacrylic acid). *Colloid and Polymer Science*, **294**, 1857-1863. https://doi.org/10.1007/s00396-016-3935-2

[15] Yoshida, E. (2015) Morphology Control of Giant Vesicles by Composition of Mixed Amphiphilic Random Block Copolymers of Poly(methacrylic acid)-*block*-poly(methyl methacrylate-*random*-methacrylic acid). *Colloid and Polymer Science*, **293**, 249-256. https://doi.org/10.1007/s00396-014-3403-9

[16] Yoshida, E. (2015) Morphological Changes in Polymer Giant Vesicles by Intercalation of a Segment Copolymer as a Sterol Model in Plasma Membrane. *Colloid and Polymer Science*, **293**, 1835-1840. https://doi.org/10.1007/s00396-015-3577-9

[17] Yoshida, E. (2015) PH Response Behavior of Giant Vesicles Comprised of Amphiphilic Poly(methacrylic acid)-*block*-poly(methyl methacrylate-*random*-methacrylic acid). *Colloid and Polymer Science*, **293**, 649-653. https://doi.org/10.1007/s00396-014-3482-7

[18] Yoshida, E. (2015) Enhanced Permeability of Rhodamine B into Bilayers Comprised of Amphiphilic Random Block Copolymers by Incorporation of Ionic Segments in the Hydrophobic Chains. *Colloid and Polymer Science*, **293**, 2437-2443. https://doi.org/10.1007/s00396-015-3679-4

[19] Yoshida, E. (2022) Polymer Nanoarchitectonics for Synthetic Vesicles with Human Erythrocyte-Like Morphology Transformation. *Colloid and Polymer Science*. (In Press) https://doi.org/10.1007/s00396-022-04958-2

[20] Yoshida, E. (2019) Perforated Giant Vesicles Composed of Amphiphilic Diblock Copolymer: New Artificial Biomembrane Model of Nuclear Envelope. *Soft Matter*, **15**, 9849-9857. https://doi.org/10.1039/C9SM01832H

[21] Yoshida, E. (2015) Fabrication of Microvillus-Like Structure by Photopolymerization-Induced Self-Assembly of an Amphiphilic Random Block Copolymer. *Colloid and Polymer Science*, **293**, 1841-1845. https://doi.org/10.1007/s00396-015-3600-1

[22] Yoshida, E. (2017) Fabrication of Anastomosed Tubular Networks Developed Out of Fenestrated Sheets through Thermo Responsiveness of Polymer Giant Vesicles. *ChemXpress*, **10**, 118. https://www.tsijournals.com/articles/fabrication-of-anastomosed-tubular-networks-developed-out-of-fenestrated-sheets-through-thermo-responsiveness-of-polymer-giant-ves.html

[23] Yoshida, E. (2021) Neuron-Like Tubule Extension of Giant Polymer Vesicles. *Chemical Reports*, **3**, 195-202. https://doi.org/10.25082/CR.2021.01.004

[24] Yoshida, E. (2018) Morphology Transformation of Giant Vesicles by a Polyelectrolyte for an Artificial Model of a Membrane Protein for Endocytosis. *Colloid and Surface Science*, **3**, 6-11. https://doi.org/10.11648/j.css.20180301.12

[25] Yoshida, E. (2014) Hydrophobic Energy Estimation for Giant Vesicle Formation by Amphiphilic Poly(methacrylic acid)-*block*-poly(alkyl methacrylate-*random*-methacrylic

acid) Random Block Copolymers. *Colloid and Polymer Science*, **292**, 2555-2561. https://doi.org/10.1007/s00396-014-3297-6

[26] Miyazawa, T., Endo, T., Shiihashi, S. and Ogawara, M. (1985) Selective Oxidation of Alcohols by Oxoaminium Salts (R2N:O+ X-). *The Journal of Organic Chemistry*, **50**, 1332-1334. https://doi.org/10.1021/jo00208a047

[27] Yoshida, E. (2013) Nitroxide-Mediated Photo-Controlled/Living Radical Polymerization of Methacrylic Acid. *Open Journal of Polymer Chemistry*, **3**, 16-22. https://doi.org/10.4236/ojpchem.2013.31004

[28] Yoshida, E. (2012) Effects of Illuminance and Heat Rays on Photo-Controlled/Living Radical Polymerization Mediated by 4-Methoxy-2,2,6,6-tetramethylpiperidine-1-oxyl. *ISRN Polymer Science*, **2012**, Article ID: 102186. https://doi.org/10.5402/2012/102186

[29] Kobayashi, S., Uyama, H., Yamamoto, I. and Matsumoto, Y. (1990) Preparation of Monodispersed Poly(methyl methacrylate) Particle in the Size of Micron Range. *Polymer Journal*, **22**, 759-761. https://doi.org/10.1295/polymj.22.759

[30] Israelachvili, J.N., Marcelja, S. and Horn, R.G. (1980) Physical Principles of Membrane Organization. *Quarterly Review of Biophysics*, **13**, 121-200. https://doi.org/10.1017/S0033583500001645

[31] Van Meer, G. (1989) Lipid Traffic in Animal Cells. *Annual Review of Cell Biology*, **5**, 247-275. https://doi.org/10.1146/annurev.cb.05.110189.001335

[32] Chapman, D. (1968) Biological Membranes. Physical Fact and Function. Academic Press, London and New York.